SCIENCE BULLETIN
CHIAO-TUNG UNIV.
Vol.3.No.2 1969

The Triangular Line Antenna

Chieh Chang*, Yung-Gunn Chen**

Abstract: -In this paper, a new form of endfire, traveling wave antenna, is described in the form of a triangular line with a corner reflector. It consists of a conductor folded into elements each of which is an equilateral triangular loop with the length of the side larger than one half wave length. The radiation patterns are measured at X-band. The endfire radiation exists over a bandwidth of approximately 21 per cent with a sidelobe level better than 20 db for 3-loops. The half power beamwidth ranges approximately from $5^{o}.1$ to $7^{o}.5$ for 5-loops.

I. Introduction

In many communication systems, we require a communication service to one fixed point only, such as communication between satellites, search radar, fire control, guided missile, etc.. In these cases, the radiation must be constrained to a narrow path as a means of conserving power and of reducing unnecessary interference with other stations. A narrow beam of radiation can be attained in many ways; array of antennas, reflector-type antennas, and traveling wave antennas are commonly used to produce a narrow beam. The principal use of the corner reflector is to reflect and focus electromagnetic energy in the direction of the bisector of the corner angle. The traveling wave antenna achieve increased gain and directivity over a single simple element by providing a structure along which the electromagnetic waves travel with a velocity equal or less than the speed of light in the medium.

The investigation of the triangular line antenna aims to improve the radiation pattern in order to increase both gain and directivity. It was developed from the slow wave structure and the corner reflector antenna. Certainly, it would contain the advantages of them. Consequently, an increase in gain and in directivity is reasonably expected. Therefore, the triangular line antenna is a kind of highly directional, traveling-wave antenna. It

* Chieh Chang is with Chung-Shan Institute of Science and Technology, Lungtan, Taiwan, Republic of China
** Yung-Gunn Chen is with Department of Electrical Engineering. Columbia University, New-York, N. Y. U.S.A

consists of a conductor folded into many equilateral triangular loops terminated at the fed end by a corner reflector. The radiation properties are characterized by the slow wave structure and the corner reflector antenna. No easy prediction can be made theoretically of the bandwidth over which the antenna would be expected to work, but this has been examined experimentally and found to be approximately 21 per cent of its center frequency of operation for 3-loops, 11 per cent for 4-loops, and 9 per cent for 5-loops, with a sidelobe level more than 20 db below the maximum main lobe. The half power beamwidths range from $5^{\circ}.9$ to $8^{\circ}.3$ for 3-loops, $5^{\circ}.4$ to $8^{\circ}.0$ for 4-loops, and $5^{\circ}.1$ to $7^{\circ}.5$ for 5-loops. Within the experimental frequency range, we find that all these results are better than the corresponding values for already existing antennas, such as Yagi, helical, zigzag or the meander line.

2. Analysis

When the triangular line antenna is fed at one end, it can be expected to launch a traveling wave of current along the structure. At the other end of the antenna this current must evidently fall to zero, and a reflected wave will thus be set up. As in the case of all other singly fed, endfire antennas, such as the Yagi or the dipole, this reflected wave is of small amplitude, and it is approximately true to say that radiation is predominatly due to the forward traveling wave alone.

Considering a single unit in the antenna as shown in Fig. 1(a), the phase difference between the adjacent loops is given by

$$\psi = kd\cos\alpha + 3B_1L - B_2d - \pi \tag{1}$$

where the π arises becuuse of the opposite directions of each adjacent loops with respect to the axis of the antenna, k is the propagation constant, B_1 and B_2 take account of the fact that the phase velocities along the loops and axis are not necessarily equal to the free space propagation constant K.

Under the endfire and the axial mode conditions, Eq. (1) becomes

$$L = \frac{(2m+1) - (k - B_2)d}{3B_1} \tag{2}$$

For $B_1 = B_2 = k$, and $m = 1$, it gives $L = \lambda_0/2$, where λ_0 is the free space wavelength. Although B_1, the propagation constant for the wave along the loops, may be assumed to be approximately k, but this is not true for B_2. The velocity along the axis of the antenna would be less than the velocity of light, because the array

of the loops acts acts effectively as a modified artificial dielectric, such as in the case of the Yagi antenna. Then from Eq. (2), $(k - B_2) < 0$ and L would be greater than $\lambda_0/2$.

By inspection of Eq. (2), it is evident that the dimension d, the spacing between the adjacent loops, may have only a minor influence in affecting the length of the side L, since the difference $(k - B_2)$ is small. When the spacing d becomes relatively large, the axial phase velocity would be expected to increase, but the difference $(k - B_2)$ would go up the other way. Thus, product $(k - B_2)$ would keep approximately constant. Therefore, if this simple relation hold, it would allow a relative flexibility in construction of the antenna.

In order to obtain an expression for the radiation pattern, the triangular line antenna may be considered as consisting of many equilateral triangular loops which of them are in linear array. Then the array factor for such n loops is given by

$$f = \frac{1}{n} \frac{\sin(\frac{n\psi}{2})}{\sin(\frac{\psi}{2})} \tag{3}$$

Note that the radiation due to connected conductors which between the adjacent loops is neglected, since its value is very small in comparison with that of the loops. The pattern factor due to the corner reflector can be obtained by the method of images and is given by

$$F = \sin(kD\cos\alpha) - \sin[kD\cos(60-\alpha)] - \sin[kD\cos(60+\alpha)] \tag{4}$$

where $D = (\frac{n+1}{2})d$

Under the above analysis, the far field pattern is then the products of the pattern of single loop, the array factor f, and the corner reflector factor F. Therefore once the pattern for the unit single loop has been found, the total far field pattern of the triangular line antenna is readily calculated.

3. Construction of the Antenna

The triangular line antenna is made of a conductor folded into many equilateral triangular loops which are arranged alternately, as displaced bow tie, shown in Fig. 1. The length of each side and the spacing between the adjacent loops are 3 cm which are required to maximize the gain and the directivity on the X-band. The corner reflector is formed by two conducting surfaces meeting at an angle of 60 degree. The axial of the triangular line coincides

with the direction of the bisector of the corner angle, and the plane of the triangular line coincides with the plane which containing the line of the bisector of the corner angle and the intersection of two surfaces, as shown in Fig. 1(e). The width and the length of the corner reflector surfaces are 12 cm and 15 cm respectively. All values of width, length and aperture angle of the corner reflector, corresponding to the dimensions of the triangular line, are also chosen for maximizing the gain and the directivity.

The single unit of the triangular line is shown in Fig. 1(a), the 3-, 4-, and 5-loops triangular line are presented in Figs. 1(b)-(d), and a 5-loops triangular line with corner reflector is shown in Fig. 1(e).

4. Measurement Techniques

The experiments were performed on the roof of a three-story laboratory building, National Chiao Tung University, Hsinchu, Taiwan, China, in the spring of 1969. The building is rectangular in shape and has a 40' x 70' yard in the center. To eliminate ground reflections, the trasmitting antenna and the receiving antenna were located on the opposite edges of the yard.

The antenna being tested was used as a receiving antenna. The target transmitting antenna, a standard horn antenna, was located approximately 40 feet away. The radiation pattern was measured by rotating the antenna being tested with an angular velocity of 0.6 rpm, around a vertical axis in the principal H-plane. The experimental set-up is shown in Fig. 17.

In the trasmitting system, a sweep generator of X-band was used to produce microwave, and a variable attenuator was used to adjust the output power level. Both frequency meter and oscilloscope were used to monitor the microwave frequency.

In the receiving system, a rotating antenna mount with 0.6 rpm or less is required, an isolator inserted between the tested antenna and the receiver was used to reduce unmatch effect, and a variable attenuator inserted ahead of the receiver was used to calibrate the measurements. Radiation pattern detected by the receiver was recorded by an X-Y recorder automatically.

Because of all equipments are in the open space of the roof of the buiding, they would be heated up by the sun light during the day, and then certain thermal noise and fluctuations due to increaing temperature occurred. In order to shun temperature effects, all experiments were undertaken at night time.

5. Experimental Results

During the tests, various shapes with different size, such as ob-

lique, right, isosceles and equilateral triangular loops as well as circular loops and square loops, were examined. Among a series of tests, we found that the equilateral triangular line having a value of both the length of the side of the triangular loops and the spacing between the adjacent loops comparable with one wavelength has the best performance both in gain and in directivity, no matter what the number of loops are.

Results of measurements are the radiation patterns, and all radiation patterns consist of a main central lobe. Some typical patterns for the H-plane at 9 GHz and 10 GHz are shown in Figs. 2-7. For the purposes of presentation and explanation, all results are arranged in a series of curves. Figs. 8-10 present the half power beamwidth as a function of frequency. Figs. 11-13 present the variations of the worst sidelobe level with frequency.

Refering to Figs. 8 9 and 10. we have

NO. of loops	Range of half power beamwidth	Maximum half power beamwidth occur at	Minimum half power beanwidth occur at
3-loops	$5^{o}.9$ to $8^{o}.3$	8.2 GHz	10 GHz
4-loops	$5^{o}.4$ to $8^{o}.0$	8.2 GHz	10 GHz
5-loops	$5^{o}.1$ to $7^{o}.5$	8.6 GHz	10.2 GHz

Refering to Fings. 11 12 and 13 we have

No. of loops	Frequency range	Sidelobe level below	center frequency	Max. side-lobe level occur at	Min. side-lobe level occur at
3-loops	10.5%	20 db	9.2 GHz	8.8 GHz	8.4 GHz
	7.5%	23 db	9.1 GHz	8.8 GHz	10.2 GHz
4-loops	5.5%	20 db	8.7 GHz	8.8 GHz	9.2 GHz
	10.6%	15 db	9.2 GHz	8.8 GHz	10.2 GHz
5-loops	4.5%	20 db	8.8 GHz	8.8 GHz	8.6 GHz
	10.5%	18 db	9.2 GHz	10.0 GHz	10.2 GHz

In general, the sidelobes are down at least 15 db and the backlobes are more than 30db below main lobe maximum for all cases. These new antennas operate satisfactory over frequency range of 8.2 GHz to 10.2 GHz and perform better than the Yagi, zigzag, and the meander line antennas in this frequency range. From Figs. 8-13, we have found that as number of loops increase the half power beamwidth becomes narrower, but the worst sidelobe level goes up the other way.

The voltage standing wave ratios of the triangular line antennas were measured with a reflecto-meter, and their variations with frequency are presented in Figs. 14-16. Although, the V. S. W. R. is not the determining factor in ascribing a bandwidth to a traveling wave antenna, but a large V. S. W. R. reduces power gain definitely.

6. Discussion

All dimensions of the triangular line antenna are purely for practical reasons and were experimentally adjusted. In the measurements, the triangular loops were uniformly distributed along the axial line of the antenna, and the spacing between the adjacent loops was an integral multiple of side length of the triangular loops. The case of which the triangular loops are nonumiformly distributed are not donsidered here but will be investigated in the near future. Probably, the more accurate information about this taiangular line antenna would be obtained in the next step.

It is not easy to obtain the expression of the exact theoretical field pattern, because how the wave traveling along the triangular line is hardly measured. Furthermore once the wave arrived at the vertex of the taiangular loop, a reflected wave will be occurred. This in turn will make the current distribution along the line more complicated and also make the calculation next to impossible. However, some important data about this antenna can be obtained by experiment. It appears from the experiments that the radiation pattern is mainly predominated by array and corner - reflector factors., the most contributions to the radiation power is due to the component of the triangular loops, and the maximum radiation power is directly proportional to the square of the ratio L/λ and inversely proportional to the square of the number of loops. It also appears that the current distribution along the axial line of the antenna is an exponentially damped sine wave. Although, the more is the number of loops, the narrower is the half power beamwidth. The bumber of loops is not unlimited, since with too many loops, sidelobe will increase both in number and in magnitude seriously.

Thus, how many number of loops is required must be determined by the degree of allowance for sidelobe.

The reflecting surfaces must be large enough to cover the whole length of the antenna, otherwise there appear many sidelobes in the radiation pattern. This result well agrees with the theoretical computation of the corner reflector antenna which almost assume that the reflecting surfaces must be infinite extent in order to apply the method of images. If the dimensions of the reflecting surfaces is not increased with the increment of the number of loops, the sidelobe level may increase.

7. Conclusions

The triangular line antenna described above is an acceptable antenna. It offers better bandwidth, narrower half power beamwidth, and lower sidelobe level than the already existing antennas, such as Yagi, helical, zigzag, and the meander line antennas, within the frequency range of 8.2 GHz to 10.2 CHz. The construction of the corner reflector is easier than that of the paraboloid. The feed system is much simpler.

Study on the possible extension of the operating frequency to this triangular line antenna other than X-band will be carried on as soon as possible.

Acknowledgement

The authors gratefully acknowledge Dr. L. J. Chu, Dr. N H. Kuo, and Prof. T. S. Wen for their helpful suggestions and illuminating discussions on the the subject of this paper. The authors would also extend their appreciation to Mr. Y. T. Chen who assisted in setting up the experiment equipment.

References

1. Edward A. Wolff "Antenna Analysis" pp. 109-115, 299-303, 372-379, Wiley, New York, (1966).
2. John D. Kraus, Ph. D. "Antenna" Chps. 4, 6, 7, 11, 12 and 15, McGraw-Hill, New York, (1950).
3. A. C. Wilson and H. R. Cottony, "Radiation Patterns of Finite-Size Corner-Reflector Antennas" IEEE On PGAP. vol. Ap-8.pp. 144-157, (1960).
4. E. F. Harris, "An Experimental Investigation of the Corner Reflector Antenna" Proc. IRE, Vol. 41, pp. 645-651, (1953).
5. T. S. M. Maclean, "The Meander Line Aerial" Electronic Engineering, pp. 667-669, (1965).

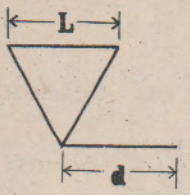

(a) Single unit of triangular line

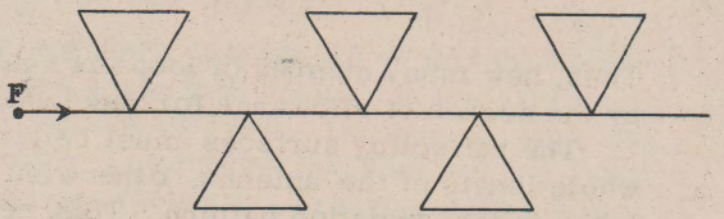

(b) Triangular line antenna 5-loop

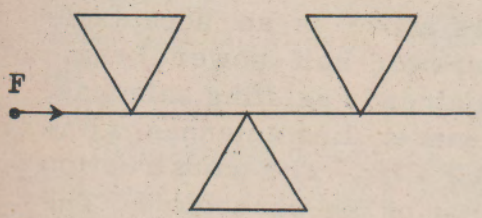

(c) Triangular line antenna 3-loop

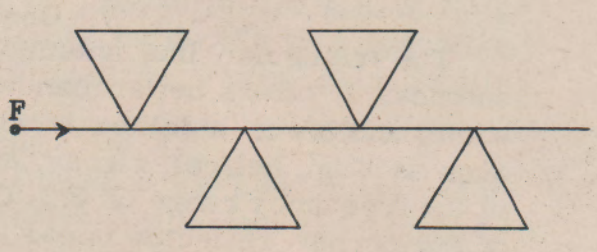

(d) Triangular line antenna 4-loop

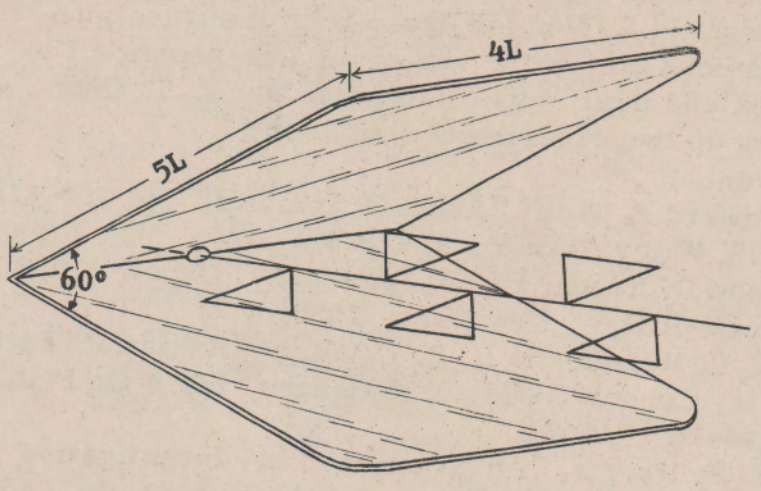

(e) Triangular line antenna with corner reflector

Fig. 1. Construction of the triangular line antenna

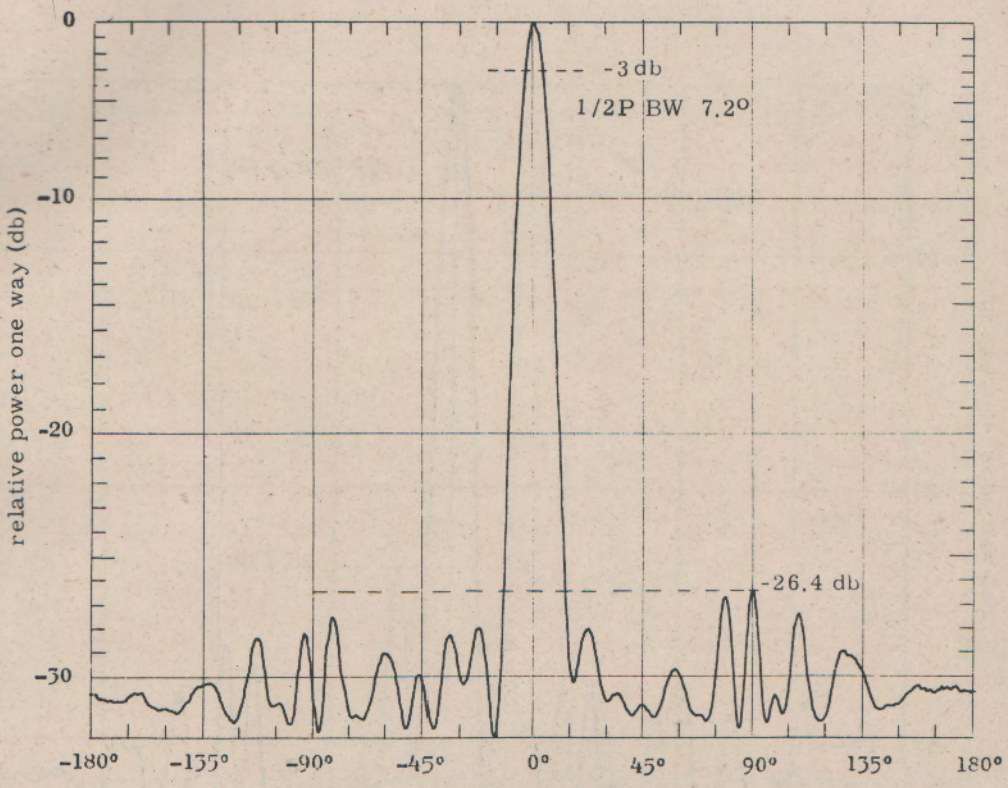

Fig. 2. H-plane pattern of 3-loop triangular line antenna at 9 GHz
($L/\lambda = 0.9$)

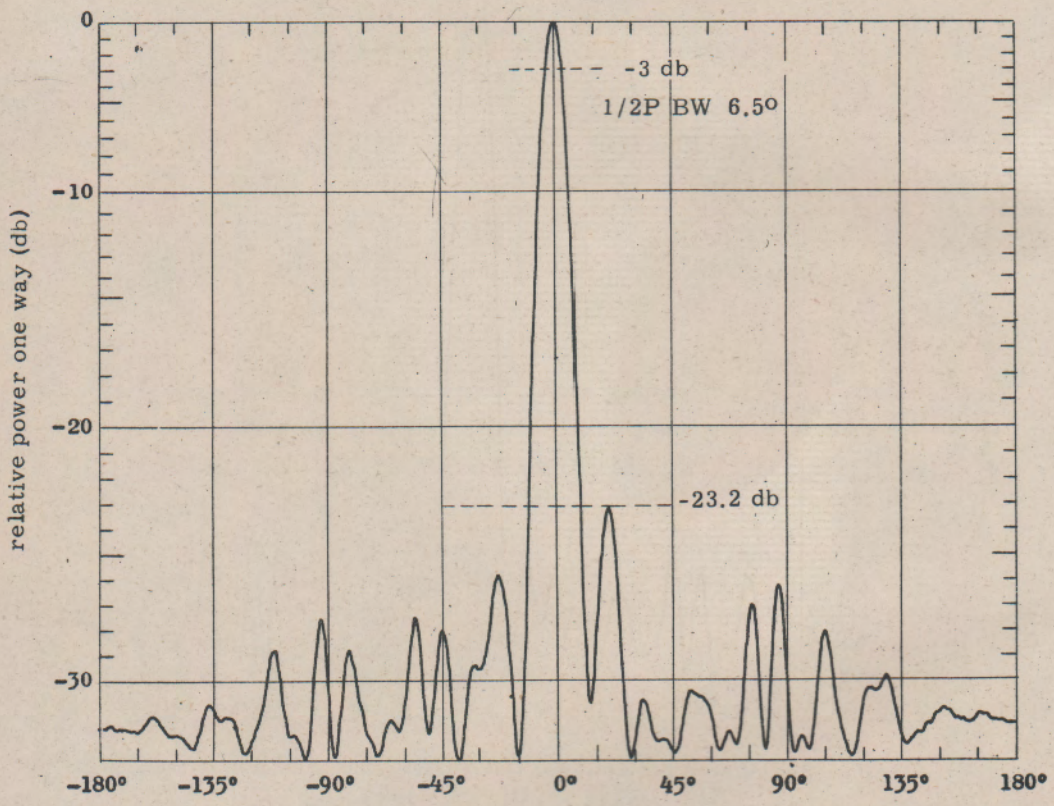

Fig. 3. H-plane pattern of 4-loop triangular line antenna at 9 GHz
($L/\lambda = 0.9$)

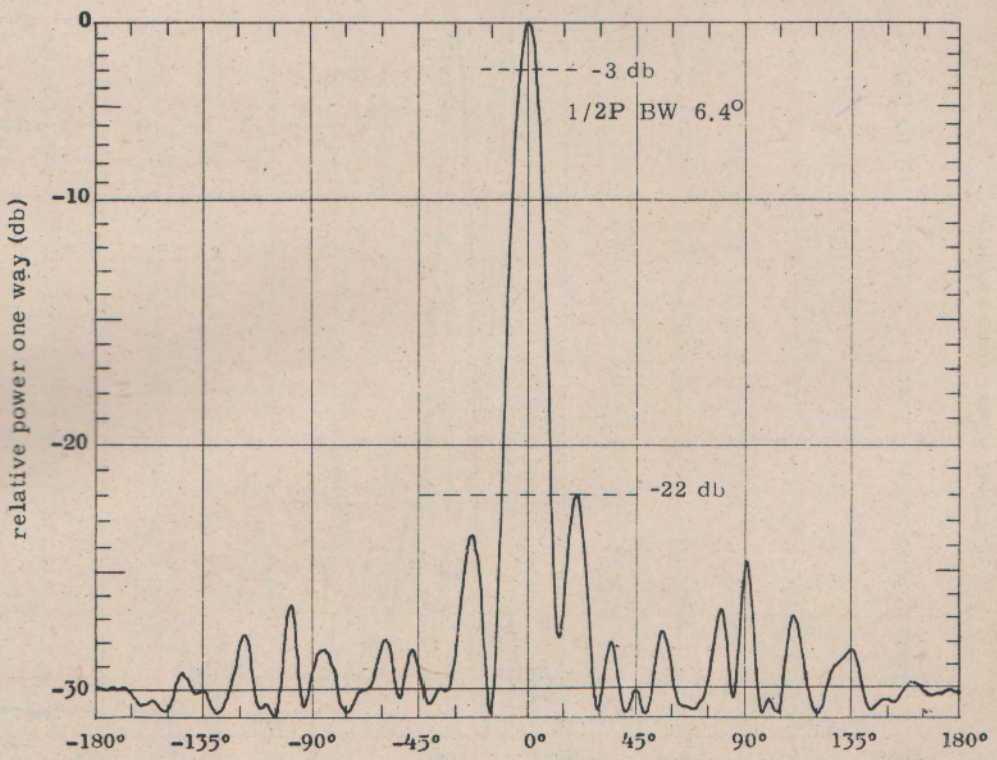

Fig. 4. H-plane pattern of 5-loop triangular line antenna at 9 GHz ($L/\lambda = 0.9$)

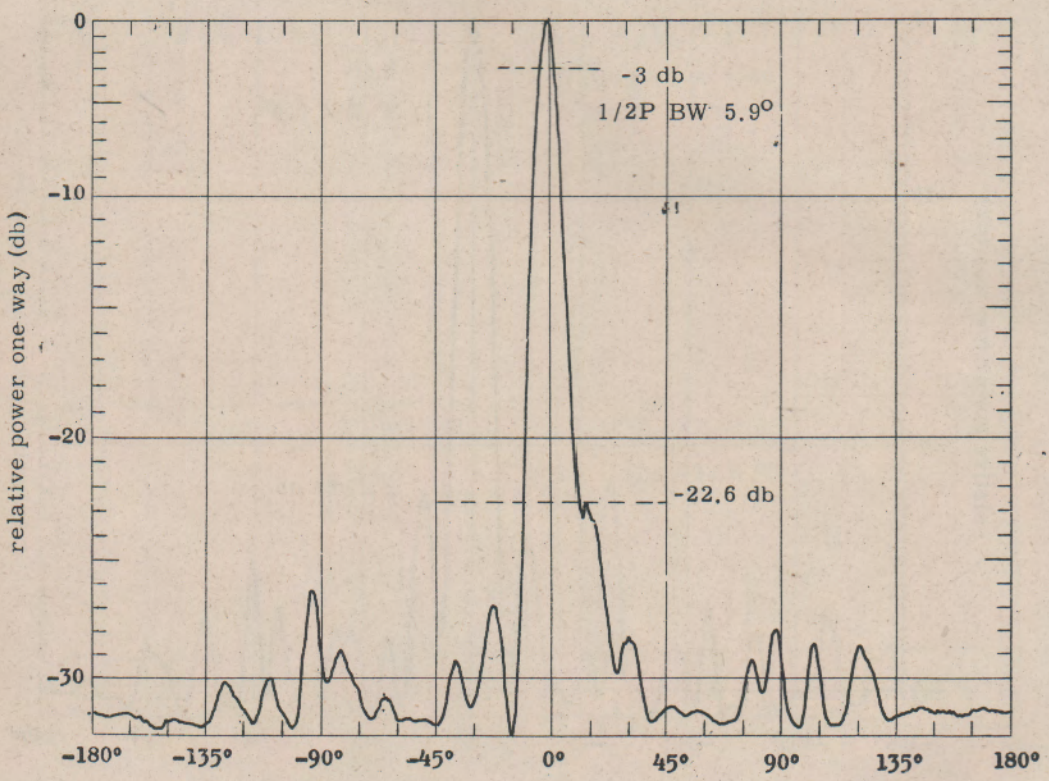

Fig. 5. H-plane pattern of 3-loop triangular antenna at 10 GHz ($L/\lambda = 1.0$)

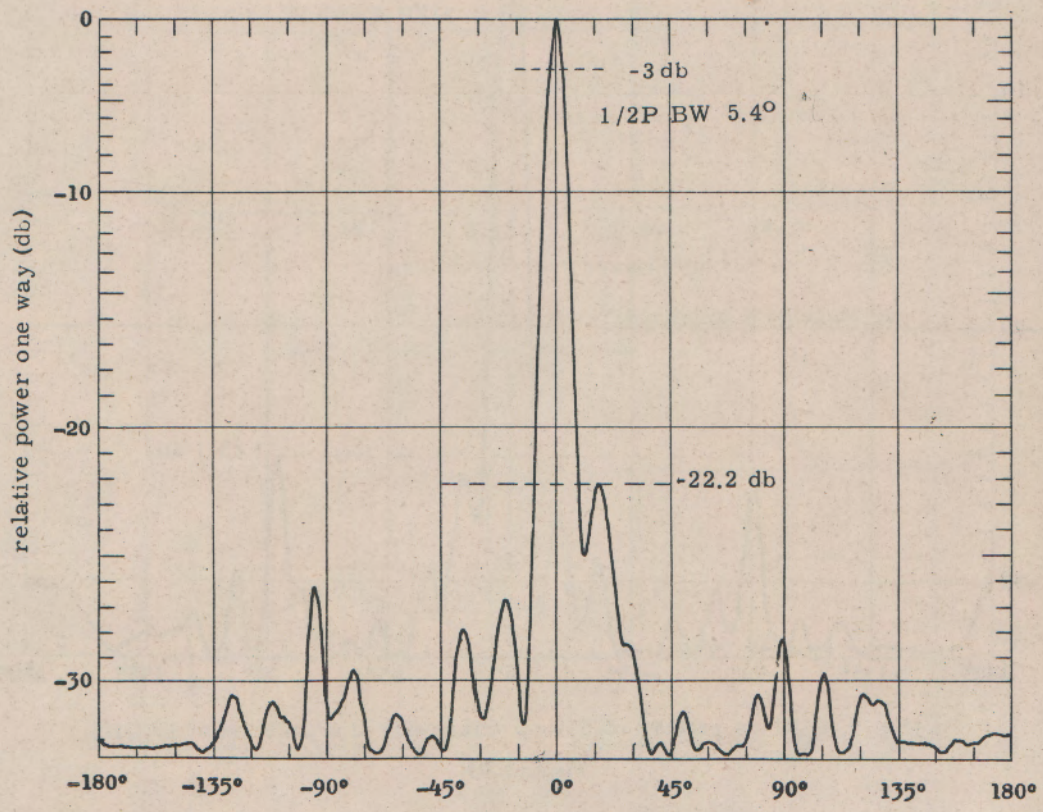

Fig. 6. H-plane pattern of 4-loop triangular line antenna at 10 GHz ($L/\lambda = 1.0$)

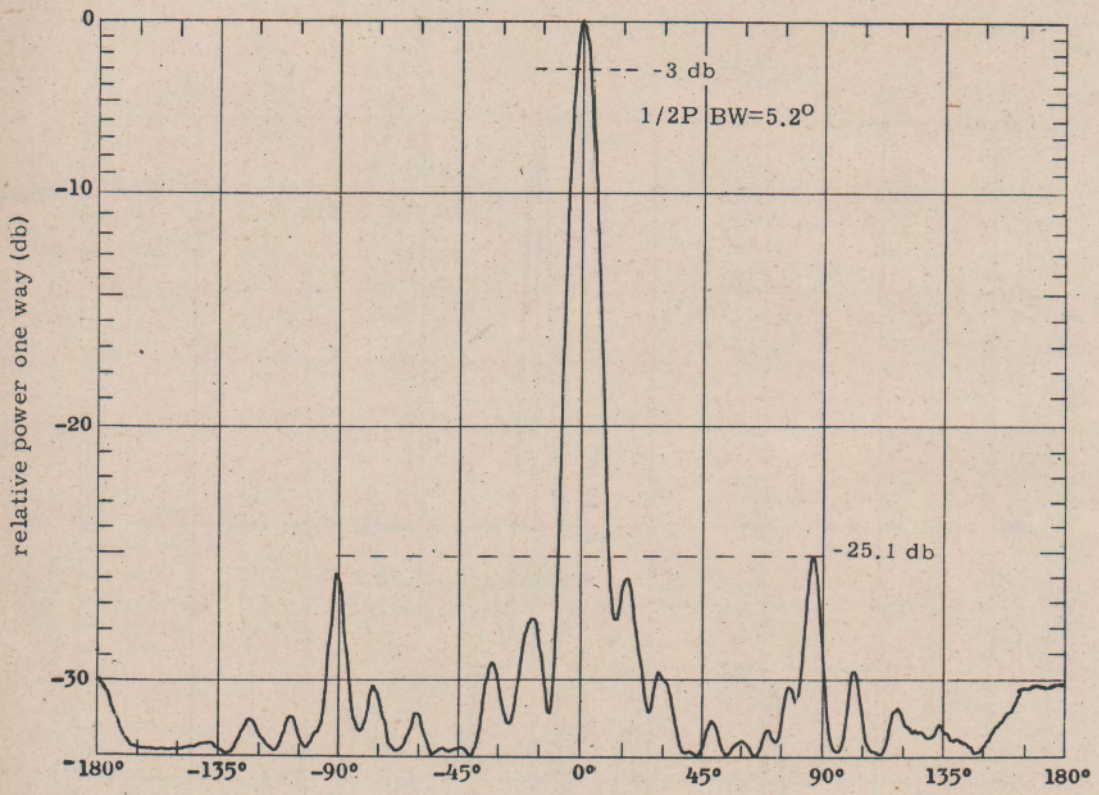

Fig. 7. H-plane pattern of 5-loop triangular line antenna at 10 GHz ($L/\lambda=1.0$)

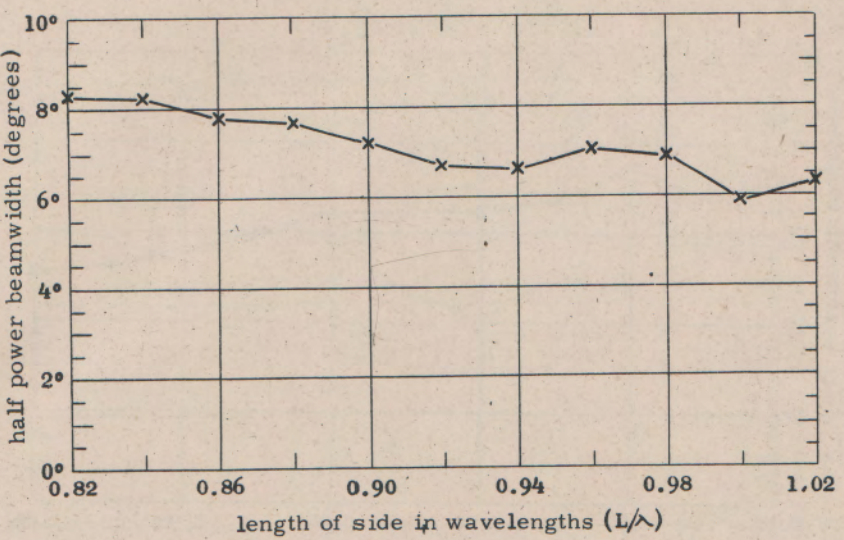

Fig. 8. Half power beamwidth as a function of frequency for 3-loop triangular line antenna

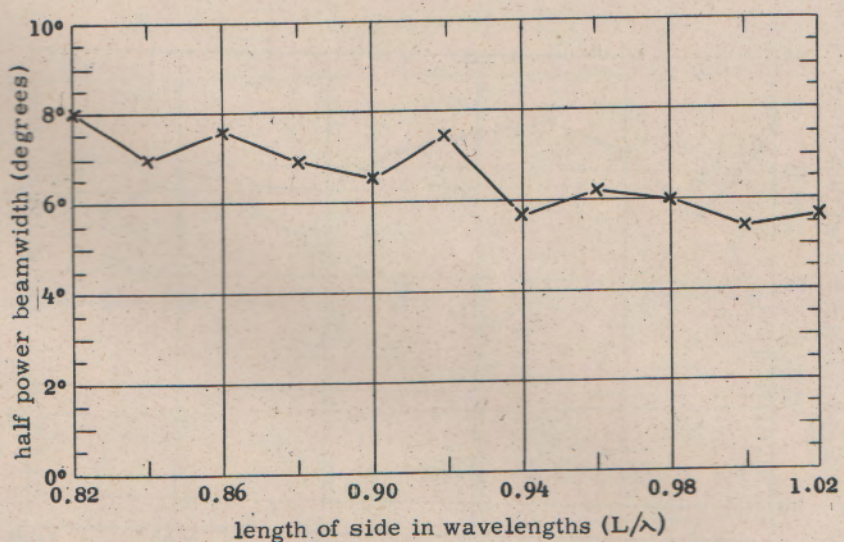

Fig. 9. Half power beamwidth as a function of frequency for 4-loop triangular line antenna

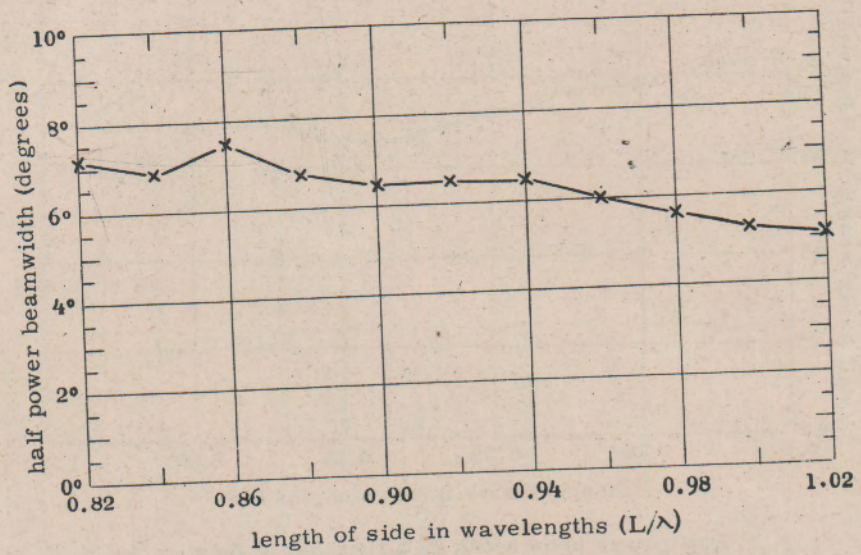

Fig. 10. Half power beamwidth as a function of frequency for 5-loop triangular line antenna

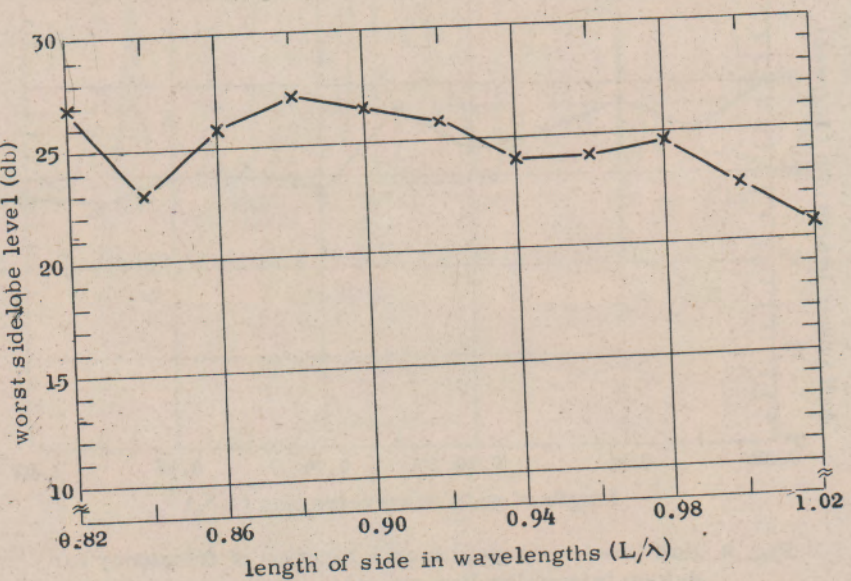

Fig. 11. Worst sidelobe level as a function of frequency for 3-loop triangular line antenna

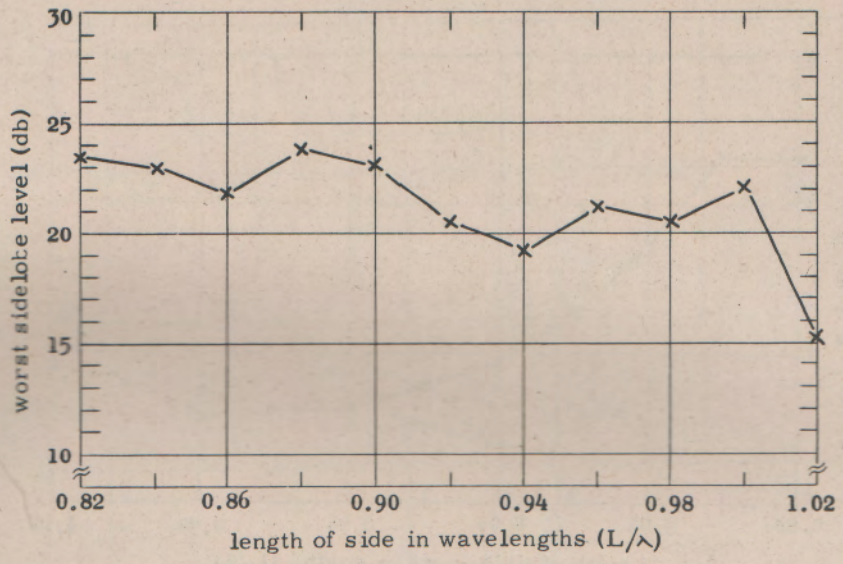

Fig. 12. Worst sidelobe level as a function of frequency for 4-loop triangular line antenna

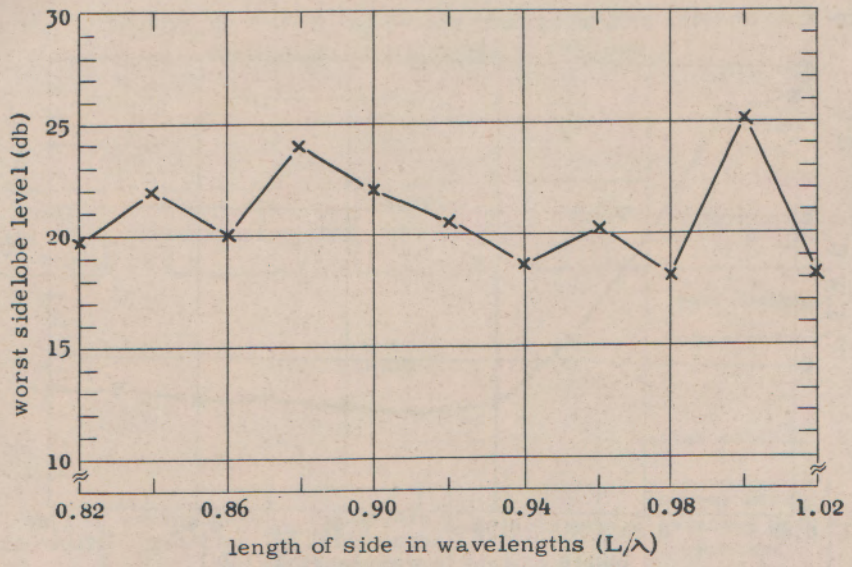

Fig. 13. Worst sidelobe level as a function of frequency for 5-loop triangular line antenna

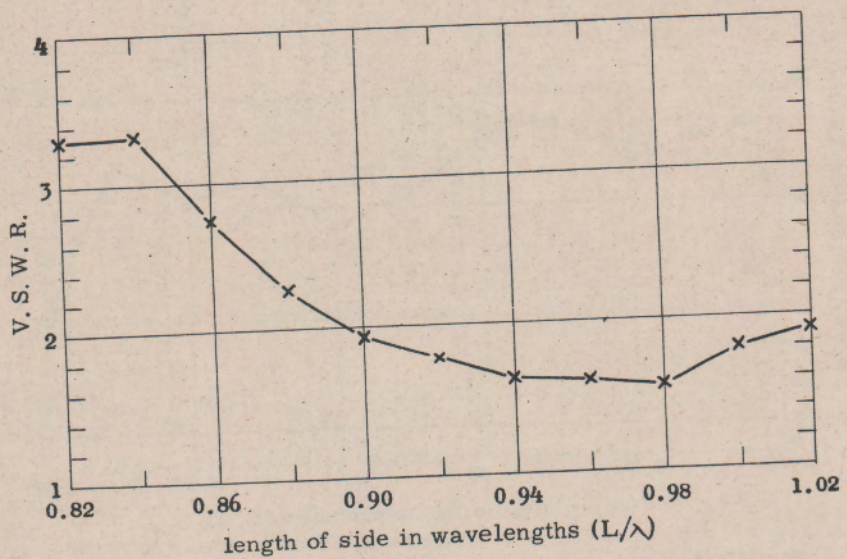

Fig. 14. V. S. W. R. of 3-loop triangular line antenna on X-band waveguide as a function of frequency

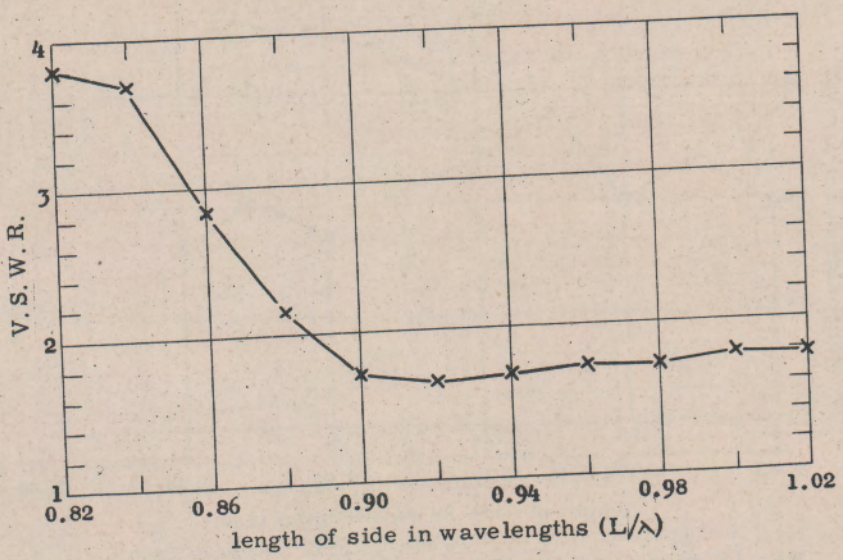

Fig. 15. V. S. W. R. of 4-loop triangular line antenna on X-band waveguide as a function of frequency

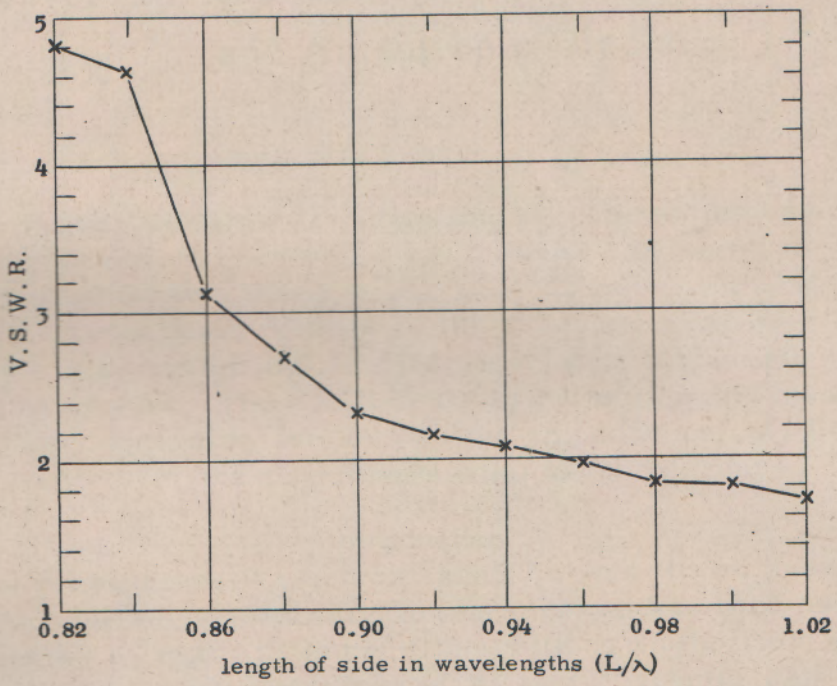

Fig. 16. V. S. W. R. of 5-loop triangular line antenna on X-band waveguide as a function of frequency

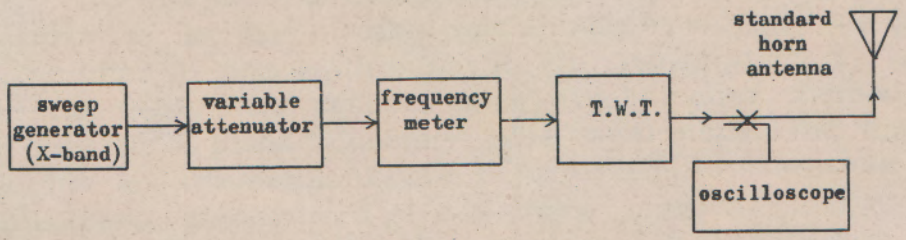

(a) Transmitting system

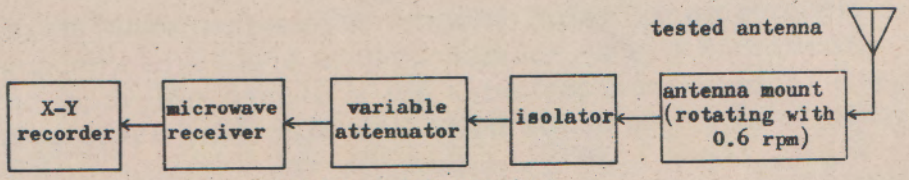

(b) Receiving system

Fig. 17. Equipments for experiment